

Dynamics of energy transport in a Toda ring

B. Sriram Shastry and A. P. Young

Physics Department, University of California, Santa Cruz, California 95064, USA

(Received 7 July 2010; revised manuscript received 20 August 2010; published 29 September 2010)

We present results on the relationships between persistent currents and the known conservation laws in the classical Toda ring. We also show that perturbing the integrability leads to a decay of the currents at long times with a time scale that is determined by the perturbing parameter. We summarize several known results concerning the Toda ring in one dimension, and present new results relating to the frequency, average kinetic and potential energy, and mean-square displacement in the cnoidal waves, as functions of the wave vector and a parameter that determines the non linearity.

DOI: [10.1103/PhysRevB.82.104306](https://doi.org/10.1103/PhysRevB.82.104306)

PACS number(s): 05.45.-a, 66.10.cd, 66.25.+g

I. INTRODUCTION

Toda's nonlinear lattice¹ is one of the very few examples of nonlinear lattices in condensed-matter physics, where explicit analytical solutions are available for the dynamics. There are several aspects of condensed-matter physics where the Toda lattice is a useful model. Toda himself applied his nonlinear lattice to understand heat propagation² and further studies with added impurities throw interesting light on this phenomenon.³ Interestingly, the lattice has also found recent applications in the context of the dynamics of DNA,⁴ where the Toda interaction is a reasonable representation of the known nonlinear couplings between base pairs. It has also been used to represent the potential of hydrogen and peptide bonds in the α helix.⁵

In this paper we study in detail the Toda lattice with periodic boundary conditions (the Toda ring). Our aim is two-fold. First we derive several noteworthy results. Second, since the Toda lattice and its properties are less well known to students of condensed matter than they deserve to be, we collect together some of the basics of the model and its solution in a form and notation that is standard in condensed-matter physics.

The excitations of this lattice are not phonons as in a harmonic lattice but can be expressed in terms of nonlinear excitations that are termed solitonic. For periodic boundary conditions the excitations are more properly the *cnoidal waves* corresponding to a family of waves characterized by a wave vector and another parameter, related to the nonlinearity of the excitations, namely, the elliptic parameter m discussed below in Sec. II A. The lattice is very simple to describe and the solution is both beautiful and instructive. Surprisingly, we find that the dispersion relation of the excitations given by Toda is only correct in the limit of weak anharmonicity or long wavelength. Here, we give a complete expression, which does not seem to have been calculated before.

Soon after Toda found the exact solution, his model was found to be exactly integrable,^{6,7} i.e., it has an infinite set of “generalized conservation laws.” These conservation laws are expressed through conserved currents that Poisson commute with the Hamiltonian as well as each other and the stability of the solitons is understood to arise from the existence of these currents.

There is considerable interest in the role of the conservation laws in the transport of heat or energy and the Toda lattice provides an excellent model to test some ideas about their role in transport, as detailed below. Since the model is classical we can study reasonably large systems (up to 64 atoms in our largest studies), unlike in quantum systems where the Hilbert space grows exponentially with the number of sites.

We address two specific issues in transport theory in this paper. The first is the role of integrability of the model in determining the exact value of the asymptotic correlation function of the energy current—this value provides us with the coefficient of the delta function in the thermal conductivity at zero frequency. It is known as the Drude term in the Kubo conductivity and is widely discussed in current literature. The second issue concerns the role of perturbations of integrable models, whereby conservation laws are destroyed. We present results on the decay of the energy current in a slightly perturbed Toda lattice for various values of the parameter that destroys integrability and show that there is an underlying scaling picture which provides a general understanding of this phenomenon.

The plan of the paper is as follows. In Sec. II A we define the Toda ring and in Sec. II B we discuss the extreme limits of harmonic and anharmonic interactions. The frequency of periodic solutions (cnoidal waves) of the Toda ring is derived in Sec. II C. In Sec. II D we highlight the differences between the results for the frequency spectrum derived in Sec. II C and the spectrum determined by Toda. We also show how, in the extreme anharmonic limit and at long wavelength, the cnoidal waves can be viewed as a train of isolated solitons. Next, in Sec. III, we calculate the kinetic energy in the modes as a function of wave vector and anharmonicity parameter, and also the ratio of the kinetic energy and the average displacement as functions of wave vector and anharmonicity. In Sec. IV we list the conserved currents of the Toda ring obtained from the Lax matrix. Next, in Sec. V, we analyze the persistence of energy currents by expanding the energy current in terms of these conserved currents. Comparing with numerical results we show that the persistent part of the conserved energy cannot be expressed in terms of the Lax currents alone but quadratic combinations of Lax currents are also needed to get an accurate description. In Sec. VI, we consider a Toda ring in which a small interaction is added which breaks integrability. We calculate numerically

the decay of the persistent currents as functions of time for different values of the perturbing parameter. We show that the results fit a scaling property that is expected but with substantial corrections to scaling so very long runs are needed to reach the asymptotic scaling regime. Finally, in Sec. VII, we summarize the main results of the paper and comment on them. Appendix A contains some needed results on elliptic functions. In Appendix B we discuss Toda’s result for the frequency spectrum ω_k^T of periodic waves, and explain why this result is only correct in some limiting cases. Appendix C gives an alternative derivation of the dispersion relation of the cnoidal waves while Appendix D computes the potential energy of the Toda ring. A slightly different version of this paper can be found on the archive.⁸

II. TODA RING, CNOIDAL WAVES, AND THEIR SPECTRUM

We summarize some interesting facts about the Toda lattice in this section. By imposing periodic boundary conditions, we deal with a ring of finite extent. The Hamiltonian of the Toda lattice is

$$H = \sum_{n=1}^N \frac{p_n^2}{2M} + \frac{a}{b} \sum_{n=1}^N \{e^{-b(u_{n+1}-u_n)} - 1 + b(u_{n+1} - u_n)\}. \quad (1)$$

The displacement variable u_n is defined through $R_n = R_n^0 + u_n$, where R_n^0 is the equilibrium position of the n th atom. In principle the displacement u_n ranges between $\pm\infty$, so for consistency, we must either imagine that the lattice constant $R_{n+1}^0 - R_n^0$ is infinite as well or that the displacements are transverse to the ring. Further we assume $u_n = u_{n+N}$ as appropriate for a ring geometry. The two nonexponential terms in the interaction potential are irrelevant since they add but a constant to the energy but it is convenient to include them since the “two-body potential” then explicitly displays a minimum at zero relative displacement. The variable p_n is conjugate to u_n satisfying the standard Poisson-Bracket relation $\{u_n, p_m\} = \delta_{n,m}$, and a, b, M are parameters.

The equations of motion follow from Hamilton’s equations

$$\dot{u}_n = \frac{p_n}{M}, \quad \dot{p}_n = -a(e^{-b(u_{n+1}-u_n)} - e^{-b(u_n-u_{n-1})}). \quad (2)$$

We note that the total momentum $p_{\text{total}} = \sum_n p_n$ is a constant of motion. The dynamics has in fact many more conservation laws, a consequence of the property of integrability which was proved by Henon⁶ and Flaschka⁷ for this system. The explicit form of the conservation laws are given later in the paper, and follow from the Lax structure that underlies the dynamics. The parameters a, b , and M give us explicit freedom to interpolate between the harmonic and extremely anharmonic limits.

A. Harmonic and anharmonic limits

A formal Taylor expansion of the exponential interaction gives us

$$H = \sum_{n=1}^N \frac{p_n^2}{2M} + \frac{\kappa}{2} \sum_{n=1}^N \left\{ (u_{n+1} - u_n)^2 - \frac{b}{3}(u_{n+1} - u_n)^3 + \frac{b^2}{12}(u_{n+1} - u_n)^4 + \dots \right\}, \quad (3)$$

where $\kappa = ab$. As long as the displacements satisfy $|u_j|b \ll 1$, the anharmonic terms do not become important so we expect a harmonic response. However for $|u_j|b \gg 1$, the anharmonic terms will dominate. To recover the harmonic lattice, one could formally take a limit $b \rightarrow 0$ and simultaneously let $a \rightarrow \kappa/b$ with κ remaining finite so that the anharmonic terms are explicitly killed.

We will see below that the cnoidal waves of Toda, contain a parameter, the elliptic “ m ” parameter, which controls the amplitude of the waves, and varying this parameter gives harmonic as well as strongly anharmonic response. Physically, the elliptic parameter m may be viewed as tuning the anharmonicity with the harmonic limit being $m \rightarrow 0$ and the extreme anharmonic limit being $m \rightarrow 1$. Mathematically, the parameter m plays a fundamental role in the theory of Jacobian elliptic functions.⁹

For later use, we note that the harmonic limit has a dispersion ω_k and sound velocity c_0 given by

$$\omega_k = c_0 2 \left| \sin \frac{k}{2} \right|, \quad c_0 = \sqrt{\frac{ab}{M}}. \quad (4)$$

B. Single-parameter formulation

The Toda lattice is also integrable in quantum theory. Quantum integrability was established by Sutherland,¹⁰ Gutzwiller,¹¹ Sklyanin,¹² and Pasquier and Gaudin¹³ using different formulations which are summarized in the work of Siddharthan and Shastry,¹⁴ who also establish their equivalence. In the viewpoint of Ref. 10 developed by Ref. 14 the Toda lattice emerges from a crystallization of a gas of impenetrable particles with an interaction $\propto \{\sinh(R_n - R_m)\}^{-2}$.

Quantum mechanically, it is possible to reduce the Toda lattice to a single-parameter problem.¹⁴ We scale $u_n \rightarrow bu_n$, $p_n \rightarrow \frac{1}{b}p_n$, $H \rightarrow \frac{1}{Mb}H$, and set $\eta = 2Ma$ so that

$$H = \sum_{n=1}^N \frac{p_n^2}{2} + \frac{\eta}{2} \sum_{n=1}^N \{e^{-(u_{n+1}-u_n)} - 1 + (u_{n+1} - u_n)\}. \quad (5)$$

In this representation $\eta \rightarrow \infty$ gives the harmonic limit since the displacements become very small so the potential energy remains small. On the other hand, $\eta \rightarrow 0$ corresponds to the extreme anharmonic limit, since now the displacements are large, and hence high order terms in the expansion of the exponential matter, and ultimately dominate. We need to keep in mind that in this extreme nonlinear limit of the model, the particles are not allowed to cross so they act as impenetrable billiard balls¹⁴ with free propagation between successive collisions. Classically, even this one parameter η

can be removed by a rescaling of the displacements so large anharmonicity corresponds to large displacements and vice versa.

C. Cnoidal wave solutions

We derive here the formulas for the excitation spectrum of the Toda ring. The relation with Toda’s work is discussed in the Appendix B. His papers^{1,2} and book¹⁵ focus on a set of dual variables and give a solution for the displacement but we point out that his dispersion relation is not appropriate for the periodic boundary conditions (i.e., a ring) which is the focus of this paper. Here we present an explicit solution for this case, which is not available in literature as far as we can tell.¹⁶ Our Eq. (41) below, concerning the total energy to mean square amplitude ratio, and related results, also seem to not have been published previously. We feel that they, too, are helpful in appreciating the Toda system from a condensed matter point of view.

The Toda Hamiltonian in Eq. (1) leads to the following equation of motion for the displacement:¹⁷

$$b\ddot{u}_n = \frac{ab}{M} \{e^{-b(u_n - u_{n-1})} - e^{-b(u_{n+1} - u_n)}\}. \quad (6)$$

We seek a special kind of solution namely a *constant profile solution*

$$bu_j(t) = d_k[\phi_j(t)],$$

$$\phi_j(t) = kj - \omega_k t = k(j - c_k t) = 2\pi \left(\frac{j}{\lambda} - \nu t \right), \quad (7)$$

where $\phi_j(t)$ is the usual phase factor depending linearly on space and time with wave vector k (or equivalently wavelength λ), and angular frequency ω_k (or equivalently frequency ν), and we have defined the velocity by $c_k = \omega_k / |k|$. We will often omit the argument of the phase for brevity. We set

$$k = \frac{2\pi}{N} \nu, \quad (8)$$

where the N integers ν obey $1 \leq \nu \leq N$. Consequently, the Brillouin zone is the range $0 \leq k \leq 2\pi$. Periodic boundary conditions, $u_n = u_{n+N}$, are satisfied if the function d_k is periodic, i.e., $d_k(x) = d_k(x + 2\pi)$. Here ω_k is yet to be determined, along with the form of d_k . We now define a scaled frequency $\bar{\omega}_k$ by $\omega_k = \sqrt{\frac{ab}{M}} \bar{\omega}_k$ so the equation of motion, Eq. (6), reduces to a nonlinear, differential, difference equation

$$\bar{\omega}_k^2 d_k''(\phi) = e^{d_k(\phi-k) - d_k(\phi)} - e^{d_k(\phi) - d_k(\phi+k)}. \quad (9)$$

This equation is satisfied by the choice

$$d_k(\phi) = \log \left\{ \frac{\theta_4\left(\frac{\phi-k}{2}\right)}{\theta_4\left(\frac{\phi}{2}\right)} \right\}, \quad (10)$$

where we summarize, in Appendix A, the necessary definitions of the elliptic theta functions as needed for this work.¹⁸

To see that Eq. (10) solves Eq. (9) we use the Jacobi addition formula for the θ functions¹⁹ and write the first term in the right-hand side (RHS) of Eq. (9) as

$$\begin{aligned} e^{d_k(\phi-k) - d_k(\phi)} &= \frac{\theta_4\left(\frac{\phi-2k}{2}\right)\theta_4\left(\frac{\phi}{2}\right)}{\theta_4^2\left(\frac{\phi-k}{2}\right)} \\ &= \frac{1}{\theta_4^2(0)} \left\{ \theta_4^2\left(\frac{k}{2}\right) - \theta_1^2\left(\frac{k}{2}\right) \frac{\theta_1^2\left(\frac{\phi-k}{2}\right)}{\theta_4^2\left(\frac{\phi-k}{2}\right)} \right\}. \end{aligned} \quad (11)$$

The second term in the RHS of Eq. (9) is obtained by replacing ϕ by $\phi+k$. Upon using the relationship between the theta functions and the Jacobian elliptic functions²⁰

$$\frac{\theta_1(x)}{\theta_4(x)} = m^{1/4} \operatorname{sn}\left(\frac{2K}{\pi}x\right), \quad (12)$$

we find the RHS of Eq. (9) is given by

$$\begin{aligned} \text{RHS Eq.(9)} &= \frac{\theta_1^2\left(\frac{k}{2}\right)}{\theta_4^2(0)} \left\{ \frac{\theta_1^2\left(\frac{\phi}{2}\right)}{\theta_4^2\left(\frac{\phi}{2}\right)} - \frac{\theta_1^2\left(\frac{\phi-k}{2}\right)}{\theta_4^2\left(\frac{\phi-k}{2}\right)} \right\}, \\ &= m^{1/2} \frac{\theta_1^2\left(\frac{k}{2}\right)}{\theta_4^2(0)} \left\{ \operatorname{sn}^2 \frac{K}{\pi} \phi - \operatorname{sn}^2 \frac{K}{\pi} (\phi-k) \right\}, \end{aligned} \quad (13)$$

where $K \equiv K(m)$ is defined in Eq. (A2). The left-hand side of Eq. (9) is

$$\frac{1}{2} \bar{\omega}_k^2 \frac{d}{d\phi} \left[\frac{\theta_4'\left(\frac{\phi-k}{2}\right)}{\theta_4\left(\frac{\phi-k}{2}\right)} - \frac{\theta_4'\left(\frac{\phi}{2}\right)}{\theta_4\left(\frac{\phi}{2}\right)} \right]$$

and, on using²¹

$$\frac{d}{dz} \left(\frac{\theta_4'(z)}{\theta_4(z)} \right) = \frac{4K^2}{\pi^2} \left[1 - \frac{E}{K} - m \operatorname{sn}^2 \frac{2Kz}{\pi} \right], \quad (14)$$

we find

$$\text{LHS Eq.(9)} = \bar{\omega}_k^2 \frac{mK^2}{\pi^2} \left\{ \operatorname{sn}^2 \frac{K}{\pi} \phi - \operatorname{sn}^2 \frac{K}{\pi} (\phi-k) \right\}. \quad (15)$$

Thus Eq. (9) is satisfied provided we assign the frequency as one of two equivalent expressions

$$\bar{\omega}_k = \frac{\pi}{m^{1/4}K} \left| \frac{\theta_1\left(\frac{k}{2}\right)}{\theta_4(0)} \right| = \frac{2}{\theta_1'(0)} \left| \theta_1\left(\frac{k}{2}\right) \right| \quad (16)$$

with the help of the following standard relations²² among Jacobi’s constants:

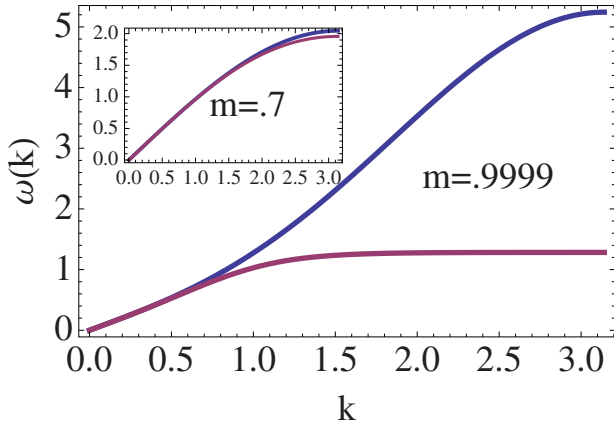


FIG. 1. (Color online) The main figure shows the dispersion relations at $m=0.9999$, which is strongly anharmonic. The inset is for $m=0.7$, which is only moderately anharmonic. The upper curve in both cases is the true spectrum, $\bar{\omega}_k$, from Eq. (16) and the lower one is $\bar{\omega}_k^T$ from Eq. (18). Except for m very close to unity, the two spectra are very close.

$$\theta_1'(0) = \theta_2(0)\theta_3(0)\theta_4(0), \quad \theta_2(0)\theta_3(0) = \frac{2}{\pi}m^{1/4}K. \quad (17)$$

Equation (16) does not appear to have been published before but an equivalent result has been obtained by Sutherland¹⁶ in unpublished notes. To summarize this section, the displacement given by the expression in Eq. (10) satisfies the equation of motion, Eq. (9), for the Toda ring with the frequency given by Eq. (16).

D. Connection between the frequency spectrum of the cnoidal waves and Toda's spectrum

Toda's result for the frequency of wavelike solutions of the Toda lattice is

$$\bar{\omega}_k^T = \frac{\pi}{K} \left\{ \frac{E}{K} - 1 + \frac{1}{\text{sn}^2\left(\frac{kK}{\pi}\right)} \right\}^{-1/2}. \quad (18)$$

The difference between our result for the dispersion relation in Eq. (16) and Toda's in Eq. (18) is shown in Fig. 1. For small m these are very close indeed, whereas for $m \rightarrow 1$ our solution always has a higher frequency. The difference between these dispersions also plays a role in determining the average potential energy as we show below in Eq. (37). As pointed out in Appendix B, the dispersion ω_k^T comes from a calculation which does not respect the boundary conditions and hence the discrepancy with our result is not surprising. Perhaps what is surprising is that they are so close for small k and differ significantly only for m close to unity.

In order to appreciate the role of the non linearity, we may usefully express the displacement and spectrum as expansions in power of the elliptic nome parameter q defined in Eqs. (A1) and (A3)

$$\bar{\omega}_k = \left| 2 \sin\left(\frac{k}{2}\right) \right| \left[\left| 1 + 4q^2 \sin^2\left(\frac{k}{2}\right) + 12q^4 \sin^2\left(\frac{k}{2}\right) \right| \right] + O(q^6),$$

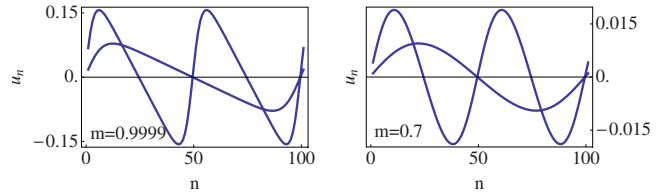


FIG. 2. (Color online) The displacements at a fixed time for different sites obtained from Eq. (10). The data is for $m=0.9999$, which is strongly anharmonic, and $m=0.7$ where the anharmonicity is weaker. Here $b=1$ and the ring is of length $N=100$. In each case, results are shown for the two smallest values of k , see Eq. (8).

$$\bar{\omega}_k^T = \left| 2 \sin\left(\frac{k}{2}\right) \right| \left[\left| 1 + 4q^2 \sin^2\left(\frac{k}{2}\right) \cos(k) + q^4 \sin^2\left(\frac{k}{2}\right) \right. \right. \\ \left. \left. \times \{6 - 5 \cos(k) + 14 \cos(2k) - 3 \cos(3k)\} \right] + O(q^6),$$

$$d_k(\phi) = 2q[\cos(\phi) - \cos(k - \phi)] + 2q^2 \sin(k)\sin(k - 2\phi) \\ + \frac{8}{3}q^3[\cos^3(\phi) - \cos^3(k - \phi)] + q^4 \sin(2k) \\ \times \sin[2(k - 2\phi)] + O(q^5). \quad (19)$$

Here we made use of the expansion of $1/\text{sn}^2$ in example 57, page 535 of Ref. 9 to rewrite Eq. (18). Note that the difference between the first two lines appears at $O(q^4)$ and is amplified for large k .

In Fig. 2 we plot the displacements at different sites, obtained from Eq. (10), for a ring of length $N=100$ at two different values of the parameter m with the lowest two k values, see Eq. (8). Notice the asymmetric shape of the displacements and their relatively broad structure.

To further visualize the periodic solution, we first note that Eq. (10) is closely related to the singly periodic Jacobi zeta function $Z(u)=Z(u+2K)$ via the relation $\frac{d}{d\phi}d_k(\phi) = \frac{K}{\pi}\{Z[\frac{K}{\pi}(\phi-k)] - Z[\frac{K}{\pi}\phi]\}$. The Jacobi zeta function has a formal Fourier series expansion, as well as one in terms of tanh. These are

$$Z(u) = \frac{\pi}{2K} \frac{\theta_4'\left(\frac{\pi u}{2K}\right)}{\theta_4\left(\frac{\pi u}{2K}\right)}, \quad (20)$$

$$= \frac{2\pi}{K} \sum_{n=1}^{\infty} \frac{q^n}{(1 - q^{2n})} \sin \frac{\pi n u}{K}, \quad \text{valid for } \Im m(u) \leq K'; \quad (21)$$

$$= -\frac{\pi}{2KK'}u + \frac{\pi}{2K'} \sum_{\nu=-\infty}^{\infty} \tanh \left\{ \frac{\pi}{2K'}(u - 2K\nu) \right\}, \quad (22)$$

where the first (second) series expansion is particularly useful in the limit $m \rightarrow 0$ ($m \rightarrow 1$).²³ The solution of the Toda lattice on a ring, i.e., the ‘‘cnoidal wave,’’ corresponds to

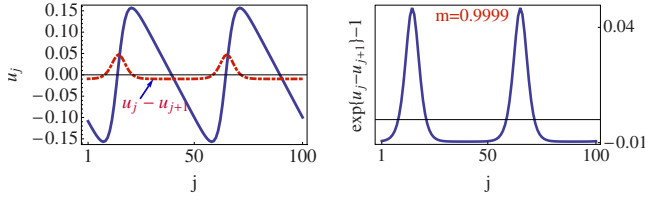


FIG. 3. (Color online) The isolation of a soliton from the cnoidal wave is illustrated here. We plot various objects for $m=0.9999$, $b=1$, and a ring length $N=100$ with $k=4\pi/N$. In the left panel we display the cnoidal wave displacements u_j and the difference between successive displacements $u_j - u_{j+1}$. In the right panel, we display the exponential of the displacement difference. The latter shows two Toda solitons, with a clear separation $\sim N/2$ and a width that is several lattice constants but much less than the separation. Note that while the displacements appear delocalized and wavelike, the solitons are quite localized and hence particlelike.

$$\begin{aligned}
 d_k(\phi) &= \frac{K}{\pi} \int_{\phi}^{\phi-k} d\phi' Z\left(\frac{K}{\pi}\phi'\right) \\
 &= -4 \sum_{n=1}^{\infty} \frac{1}{n} \frac{q^n}{1-q^{2n}} \sin n\left(\phi - \frac{k}{2}\right) \sin n\frac{k}{2} \\
 &= \frac{K}{4\pi K'} (2\phi - k)k + \sum_{\nu=-\infty}^{\infty} \log \left[\frac{\cosh \frac{K}{2K'} \{\phi - k - 2\pi\nu\}}{\cosh \frac{K}{2K'} \{\phi - 2\pi\nu\}} \right].
 \end{aligned} \tag{23}$$

The last line follows from using the Poisson summation formula to rewrite the second line.²³

Let us comment on the limit when the elliptic parameter m tends to 0, where the second line in Eq. (23) is useful. It is easily seen that we obtain the harmonic excitations in this limit. Using the standard expansion of the various objects in m , the displacement is given by $u_j = \frac{m}{8b} [\cos(\phi_j) - \cos(\phi_j - k)]$, and the prefactor of m makes these small amplitude oscillations. The spectrum is also that of the harmonic limit, since Eq. (16) becomes $\bar{\omega}_k = 2|\sin \frac{k}{2}|$ and the phase factor in Eq. (7) is given by $\phi_j = k(j - c_k t)$ with velocity $c_k = \sqrt{ab/M} = c_0$, as expected from Eq. (4).

In the other extreme limit of the elliptic parameter, $m \rightarrow 1$, the elliptic functions degenerate into hyperbolic functions and the cnoidal wave is regarded as a train of solitons so that the periodicity of the displacements around the ring is unimportant. This is illustrated in Fig. 3, where we plot, for a typical case, the displacements u_j , their nearest-neighbor differences $u_j - u_{j+1}$, and the exponential of the latter, i.e., $\exp\{u_j - u_{j+1}\}$.

Let us now extract a single isolated soliton from the solution. We start with Eq. (D1) for the exponential of the displacement difference in terms of sn^2 and using $\text{dn}^2(u) = 1 - m \text{sn}^2(u)$, Eq. (22) and the relation $\frac{d}{du} Z(u) = \text{dn}^2(u) - E/K$, we find a useful and formally exact series representation^{1,2,15}

$$e^{bu_j - bu_{j+1}} = A + \bar{\omega}_k^2 \left(\frac{K}{2K'}\right)^2 \sum_{\nu=-\infty}^{\infty} \text{sech}^2 a \frac{K}{\pi} [\phi_j(t) - 2\pi\nu], \tag{24}$$

where $a = \frac{\pi}{2K'}$ and

$$A = \left(\frac{\bar{\omega}_k K}{\pi}\right)^2 \left\{ \frac{\text{cn}^2\left(\frac{kK}{\pi}\right)}{\text{sn}^2\left(\frac{kK}{\pi}\right)} + \frac{E - a}{K} \right\}.$$

The periodicity in the phase angle $\phi \rightarrow \phi + 2\pi\nu$ is manifest in this way of writing the displacement difference.

Let us focus on $m \rightarrow 1$ so that we may set $K' \rightarrow \pi/2$ and $a \rightarrow 1$. With $\phi_j(t) = kj - c_0 \bar{\omega}_k t$, we observe that the separation Δj between peaks of the exponential of displacement difference Eq. (24), is $2\pi/k$. We shall see in Eq. (32) below that the width of these peaks is given by κ^{-1} where

$$\kappa = \frac{1}{\pi} kK \tag{25}$$

and so the requirement that the separation between the peaks is much greater their separation is

$$K \gg 1, \quad \text{or equivalently} \quad 1 - m \ll 1. \tag{26}$$

It is clearly necessary that the width of the peak is at least several lattice spacings and so we also need the condition $\kappa \leq 1$. Combining with Eqs. (25) and (26) the condition for the oscillations to be described by well separated solitons is

$$k \leq K^{-1} \ll 1, \tag{27}$$

which, as shown in Eq. (26), implies that m is very close to 1, i.e., the system is in the extreme anharmonic limit.

In the proximity of a peak, we drop the sum over ν , set $A \rightarrow 1$,²⁴ and write

$$e^{b(u_j - u_{j+1})} = 1 + \bar{\omega}_k^2 \left(\frac{K}{\pi}\right)^2 \text{sech}^2 \left[\left(\frac{K}{\pi}\right) (kj - c_0 \bar{\omega}_k t) \right]. \tag{28}$$

From Eq. (16), $\theta_1(k/2)$ determines the dispersion, and in the expression (A5), the first few terms in an expansion for positive k read as

$$\bar{\omega}_k = \frac{2K'}{K} e^{-k^2 K/K'} \left[\sinh \frac{kK}{2K'} - e^{-2\pi(K/K')} \sinh \frac{3kK}{2K'} \right]. \tag{29}$$

As $m \rightarrow 1$, K is large and $K' \rightarrow \pi/2$, and in the regime $kK \leq 1$ which is well satisfied here, see Eq. (27), we may further approximate this by writing

$$\bar{\omega}_k = \frac{\pi}{K} \sinh \left(\frac{kK}{\pi} \right). \tag{30}$$

The same answer is also found from Toda's relation Eq. (18), since k is small enough in this regime that the distinction between the two dispersions is negligible. In terms of the parameter κ defined in Eq. (25) above and calling the soliton velocity

$$c_\kappa = c_0 \frac{\sinh \kappa}{\kappa}, \quad (31)$$

where $c_0 = \sqrt{\frac{ab}{M}}$, we find

$$e^{b(u_j - u_{j+1})} - 1 = \frac{\sinh^2 \kappa}{\cosh^2[\kappa(j - c_\kappa t)]}. \quad (32)$$

Equation (32) is the profile of the famous Toda soliton, two of which are seen in the right panel of Fig. 3. We see that the soliton parameter κ controls the amplitude of the solitons [through the prefactor in the amplitudes $\sinh^2(\kappa)$], the velocity c_κ and also the length scale of spatial variation $\frac{1}{\kappa}$. Since $\frac{\sinh \kappa}{\kappa} \geq 1$, the velocity of the soliton c_κ in Eq. (31) is always greater than the sound velocity c_0 .

For completeness we note the displacement for an isolated soliton, by using the same limits as above in Eqs. (26) and (27). The displacement u_j and its time derivative can be written from Eq. (23), where we retain only $\nu=0$ (since $K \gg 1$) and write

$$u_j \sim \frac{1}{b} \log \left[\frac{\cosh \kappa(j - 1 - c_\kappa t)}{\cosh \kappa(j - c_\kappa t)} \right], \quad (33)$$

$$\dot{u}_j \sim \frac{c_0 \sinh \kappa}{b} [\tanh \kappa(j - c_\kappa t) - \tanh \kappa(j - 1 - c_\kappa t)]. \quad (34)$$

It is now straightforward to see that the equation of motion Eq. (6) is satisfied by the single soliton solution given in Eqs. (32)–(34). Toda notes that if we ignore the periodic boundary conditions, and imagine Eqs. (32)–(34) to be extended for all $-\infty \leq j \leq \infty$, then integrating Eq. (33) gives $u_\infty - u_{-\infty} = \frac{2\kappa}{b}$, so there is a net compression near the soliton. Hence the soliton can be regarded as a local compression propagating with speed c_κ given by Eq. (31).

The momentum $M\dot{u}_j$ vanishes at $j \rightarrow \pm \infty$, as does the potential energy term Eq. (32). Therefore the energy of a soliton, obtained by ignoring periodic boundary conditions and opening the ring into an infinite chain, is finite. Substituting for \dot{u}_j and the displacement difference from Eqs. (33) and (34) into the Hamiltonian Eq. (1), and with $p_j = M\dot{u}_j$, we obtain this energy to be $\epsilon_{\text{Soliton}} = \frac{2a}{b} (\sinh \kappa \cosh \kappa - \kappa)$.

With the Fourier expansion in Eq. (23) one can give an alternate derivation of the dispersion relation of the Toda lattice with periodic boundary conditions in Eq. (16). This is done in Appendix C.

III. ENERGY OF CNOIDAL WAVES

We next turn calculate the total energy of the Toda ring with a cnoidal wave. As a prelude, let us recapitulate the results of the trivial harmonic lattice with the Hamiltonian in Eq. (3) truncated at the quadratic level. If we assume a phonon displacement $u_n = u_0 \sin(kn - \omega_k t)$, then $\omega_k = \sqrt{\frac{\kappa}{M}} |2 \sin \frac{k}{2}|$. The cycle average of the total kinetic energy and potential energy at wave vector k are easily found to be

$$\overline{\text{KE}} = \overline{\text{PE}} = Nu_0^2 \kappa \sin^2 \frac{k}{2},$$

$$\rho \equiv \frac{\overline{\text{KE}}}{\overline{u_n^2}} = \frac{1}{2} NM \omega_k^2 = \frac{1}{2} Nab \left| 2 \sin \frac{k}{2} \right|^2. \quad (35)$$

We next calculate the kinetic energy of the Toda ring using the cnoidal wave solution Eq. (23) as a Fourier series. Let us start with the kinetic energy expression

$$\begin{aligned} \text{KE} &= \frac{M}{2} \sum_j (\dot{u}_j)^2 = \frac{M \omega_k^2}{2b^2} \sum_j \{d'_k[\phi_j(t)]\}^2, \\ \overline{\text{KE}} &= 4N \left(\frac{a}{b} \bar{\omega}_k^2 \right) \sum_{n=1}^{\infty} \frac{q^{2n}}{(1 - q^{2n})^2} \sin^2 n \frac{k}{2}. \end{aligned} \quad (36)$$

Here we used Eq. (7) and the last line is obtained by taking the time average over a cycle with the displacement from the series in Eq. (23).

The potential energy of the Toda ring, averaged over a cycle, is calculated in Appendix D, where we show that

$$\overline{\text{PE}} = N \frac{a}{b} \left[\left(\frac{\bar{\omega}_k}{\bar{\omega}_T} \right)^2 - 1 \right]. \quad (37)$$

We expand Eq. (37), as in Eq. (19) in terms of the nome “ q ” to lowest order and find

$$\overline{\text{PE}} = N \frac{a}{b} \left[16q^2 \sin^4 \left(\frac{k}{2} \right) (1 + 6q^2) + O(q^6) \right]. \quad (38)$$

We now compute the ratio of kinetic to potential energies, and express it as a series in the nome

$$\frac{\overline{\text{KE}}}{\overline{\text{PE}}} = 1 + 4q^2 \sin^2 \left(\frac{k}{2} \right) + O(q^4), \quad (39)$$

which is unity for small anharmonicity, as expected, and increases above unity for greater anharmonicity.

In fact, we shall mainly compute the Fourier series for the mean-square displacement

$$u_j = \frac{1}{b} d_k[\phi_j(t)],$$

$$\overline{u_j^2} = \frac{8}{b^2} \sum_{n=1}^{\infty} \frac{1}{n^2} \frac{q^{2n}}{(1 - q^{2n})^2} \sin^2 n \frac{k}{2} = \frac{2}{b^2} \int_0^{kK/2\pi} dy y \xi \left(\frac{kK}{2\pi} - y \right), \quad (40)$$

where $\xi(u) = \int_0^{2K} \frac{dv}{2K} Z(v) Z(u+v)$.²⁵ Combining Eqs. (36) and (40), we find the total energy to mean-square amplitude ratio

$$\rho \equiv \frac{\overline{\text{KE}}}{\overline{u_j^2}} = \frac{1}{2} (NM \bar{\omega}_k^2) \frac{\sum_{n=1}^{\infty} \frac{q^{2n}}{(1 - q^{2n})^2} \sin^2 n \frac{k}{2}}{\sum_{n=1}^{\infty} \frac{1}{n^2} \frac{q^{2n}}{(1 - q^{2n})^2} \sin^2 n \frac{k}{2}} \quad (41)$$

with Eq. (16) defining the spectrum $\bar{\omega}_k$.

We can express the average kinetic energy in a more compact form using the expression in Eq. (11) for the displacements. Let us write

$$\begin{aligned} \overline{\text{KE}} &= -\frac{M}{2} \sum_j \overline{\ddot{u}_j u_j} = \frac{Na}{2b} \frac{\omega_k}{2\pi} \int_0^{2\pi/\omega_k} \\ &\quad \times dt \{d_k(\phi - k) - d_k(\phi)\} e^{i\{d_k(\phi-k) - d_k(\phi)\}} \\ &= \frac{Na}{2b} \alpha_k \int_0^{2K} \frac{du}{2K} \left(\text{dn}^2 u - \frac{E}{K} \right) \log \left[1 + \alpha_k \left(\text{dn}^2 u - \frac{E}{K} \right) \right], \end{aligned} \quad (42)$$

where we have set $\alpha_k = \bar{\omega}_k^2 \frac{K^2}{\pi^2}$ and used Eq. (D1). This expression is particularly useful if we want long wavelength results since we can expand in α_k and find the exact elliptic parameter (i.e., m) dependent coefficients. The leading term for long wavelengths [up to and including $O(k^4)$] is

$$\begin{aligned} \overline{\text{KE}} &= \frac{Na}{2b} \alpha_k^2 \left[\int_0^K \frac{du}{K} \text{dn}^4 u - \frac{E^2}{K^2} \right] + O(k^4) \\ &= \frac{Na}{2b} \alpha_k^2 \left[\frac{2}{3} (2-m) \frac{E}{K} - \frac{1}{3} (1-m) - \left(\frac{E}{K} \right)^2 \right] + O(k^4), \\ &\sim \begin{cases} \frac{Na}{2b} \alpha_k^2 \left[\frac{m^2}{8} - \frac{m^4}{1024} \right] & (m \rightarrow 0) \\ \frac{Na}{2b} \alpha_k^2 \left[\frac{4}{3 \log \frac{16}{1-m}} \right] & (m \rightarrow 1). \end{cases} \end{aligned} \quad (43)$$

We can also extract the long wavelength behavior of Eq. (40) using²⁶ as

$$\begin{aligned} \overline{u_j^2} &= \frac{2}{b^2} k^2 \sum_{n=1}^{\infty} \frac{q^{2n}}{(1-q^{2n})^2} + O(k^4) \\ &= \frac{2}{b^2} k^2 \left[\frac{1}{24} + \frac{1}{6} (2-m) \frac{K^2}{\pi^2} + \frac{EK}{2\pi^2} \right] \\ &\sim \begin{cases} \frac{2}{b^2} k^2 \left[\frac{m^2}{256} \right] + O(k^4) & (m \rightarrow 0) \\ \frac{2}{b^2} k^2 \left\{ \frac{[\log(1-m)]^2}{24\pi^2} \right\} & (m \rightarrow 1). \end{cases} \end{aligned} \quad (44)$$

We finally put together the results for the kinetic energy and the mean-square amplitude to form the ratio

$$\rho = \frac{1}{2} N(ab) k^2 \left[1 + \frac{3}{256} (m^2 + m^3) + O(m^4) \right], \quad (m \rightarrow 0), \quad (45a)$$

$$\rho = N(ab) k^2 \frac{\log(16)^3}{2\pi^2} \log \frac{1}{1-m}, \quad (m \rightarrow 1). \quad (45b)$$

We see that the small m limit of Eq. (45a) gives the long-wavelength limit of the harmonic lattice result given in Eq. (35). In the opposite, strongly anharmonic, limit the kinetic energy grows logarithmically as $m \rightarrow 1$.

IV. CONSERVED CURRENTS OF THE TODA RING

We summarize in this section the construction of the conservation laws of the Toda lattice, and write out explicitly the

first few conservation laws. For brevity we set $m=a=b=1$. The work of Henon⁶ and Flaschka⁷ gives us a construction of the conservation laws starting with the Lax equation $\dot{L} = [L, A]$, where L and A are $N \times N$ matrices with entries

$$L_{n,m} = \delta_{n,m} p_n + \chi_{n,m},$$

$$\chi_{n,m} = i \{ \delta_{m,n+1} e^{-1/2(u_m - u_n)} - \delta_{m,n-1} e^{-1/2(u_n - u_m)} \},$$

$$A_{n,m} = -i/2 \{ \delta_{m,n+1} e^{-1/2(u_m - u_n)} + \delta_{m,n-1} e^{-1/2(u_n - u_m)} \} \quad (46)$$

so that the Lax equation leads to the original equation of motion, Eq. (2). Further, we can construct N -independent conservation laws by taking the trace of the first N powers of the Lax matrix. With the definition

$$J_n = \frac{1}{n!} \text{Tr} L^n; \quad 1 \leq n \leq N \quad (47)$$

it has been shown that these are in mutual involution,^{1,6,7} i.e., their Poisson brackets are all zero, $\{J_n, J_m\} = 0$, and thus they form a complete set of independent conservation laws. We list the first few conservation laws

$$J_1 = p_{\text{total}}, \quad (48a)$$

$$J_2 = H + \text{const.}, \quad (48b)$$

$$J_3 = \frac{1}{6} \sum_n p_n^3 + \frac{1}{2} \sum_n p_n \{ e^{(u_n - u_{n+1})} + e^{(u_{n-1} - u_n)} \}, \quad (48c)$$

$$\begin{aligned} J_4 &= \frac{1}{24} \sum_n p_n^4 + \frac{1}{6} \sum_n p_n^2 \{ e^{(u_n - u_{n+1})} + e^{(u_{n-1} - u_n)} \} \\ &\quad + \frac{1}{6} \sum_n p_{n+1} p_n e^{(u_n - u_{n+1})} + \frac{1}{6} \sum_n e^{(u_n - u_{n+2})} + \frac{1}{12} \sum_n e^{2(u_n - u_{n+1})}. \end{aligned} \quad (48d)$$

We make extensive use of these conservation laws in later sections.

V. PERSISTENCE OF ENERGY CURRENT AND ITS RELATIONSHIP TO CONSERVED CURRENTS

In this section we study the decay and persistence of the energy current in the Toda lattice with periodic boundary conditions. The energy current is obtained from the energy-density conservation law $\dot{H}(x, t) + \partial_x J_E(x, t) = 0$, with a suitable discretization of the spatial derivative. To obtain the energy current, we write $H = \sum_j p_j^2 / (2M) + \frac{1}{2} \sum_{i,j} V_{i,j}$, where $V_{i,j} = V(u_i - u_j) = \frac{a}{b} e^{-b(u_i - u_j) \eta(i,j)}$ and $\eta(i, j) = (j - i) \delta_{1, |i-j|}$. The constant and linear term in Eq. (1) can be omitted safely since they do not change the current. Thus the force on atom i due to atom j is

$$F_{i,j} = -\partial_{u_i} V_{i,j} = a \eta(i, j) e^{-b(u_i - u_j) \eta(i, j)}.$$

We note the symmetry $V_{i,j} = V_{j,i}$ and $F_{i,j} = -F_{j,i}$. Thus we write $H = \sum_i H_i$ with $H_i = p_i^2 / (2M) + \frac{1}{2} \sum_j V_{ij}$, and therefore de-

noting $v_i = p_i/M$, the rate of change in local energy is given by

$$\begin{aligned} \dot{H}_i &= v_i \dot{p}_i - \frac{1}{2} \sum_j F_{i,j}(v_i - v_j) = \frac{1}{2} \sum_j F_{i,j}(v_i + v_j) \\ &= \frac{1}{2} F_{i,i+1}(v_i + v_{i+1}) - F_{i-1,i}(v_i + v_{i-1}) = -J_E(i+1) + J_E(i). \end{aligned} \quad (49)$$

Therefore we may write alternate expressions for the energy current that are equivalent

$$J_E = \frac{1}{2} \sum_i F_{i-1,i}(v_i + v_{i-1}), \quad \text{or} \quad J_E = \frac{1}{2} \sum_i v_i (F_{i-1,i} + F_{i,i+1}) \quad (50)$$

with $F_{i-1,i} = -ae^{-b(u_i - u_{i-1})}$. We use the second form of the current above, and will set $M = a = b = 1$ in Hamiltonian (1) in the sequel.

We compute the correlation function

$$C_{J_E}(t) = \langle J_E(t) J_E(0) \rangle, \quad (51)$$

where the average is taken in the canonical ensemble. This function does not decay to zero at long times but rather reaches a finite value. This is the phenomenon of temporal persistence and is related to the integrability of the underlying model. The implication of this nonvanishing of $C(t \rightarrow \infty)$ is that the Fourier transform of $C(t)$, namely the Kubo thermal conductivity, contains a Dirac delta function at zero frequency $\delta(\omega)$. Thus the thermal conductivity has a Drude term in common with many other integrable models studied in recent years.

Inspired by Mazur,²⁷ we assume that the time integrated energy current can be written as a linear combination of all the conserved quantities of the model I_n

$$\lim_{t \rightarrow \infty} \frac{1}{t} \int_0^t J_E(t') dt' = \sum_n a_n I_n \quad (52)$$

for fixed coefficients a_n . Both sides of this equation depend on the initial state of the system. Again following Mazur, we argue that it holds, with the same a_n , for almost all initial states on a constant energy surface. Here we will test Eq. (52) for different initial states from a *canonical distribution*. The set of constants of motion I_n are not spelled out in detail in earlier work, although one expects that these are *functions* of the independent currents J_n in Eq. (47).

Using Eq. (52), and a few chosen conserved currents, one can obtain a *lower bound* to the persistent part of the current-current correlations.²⁷ The nice thing about this result is that even a single nontrivial conserved current could help establish the existence of the temporal persistence.²⁸ While in most applications of this idea, one has to be content with the result as a *bound*, one would also like to test the idea of completeness, i.e., to see if the bound is saturated in a case where one has a full knowledge of the conservation laws. A natural expectation is that if *all* the conserved currents that go into this expansion are known, then we should be able to get the exact value of the persistent part of the correlations.

This is the operator analog of expanding vectors in a complete basis. Mazur gives the example of the XY model of magnetism in one dimension,²⁹ where all the higher conservation laws are known in the quantum theory, since the problem is reducible to free fermions. In that case, he points out that exact persistent part of correlations can be obtained from a knowledge of these conservation laws. Initially, we will test the hypothesis that the set of conservation laws coincides with the constants of motion found in Eq. (47), i.e., we begin by assuming that $I_n = J_n$. Later, we will discover that one needs to expand the set I_n to include further terms, such as bilinears in the J_n .

We begin by determining the a_n in terms of thermally averaged correlation functions. Multiplying Eq. (52) (with $I_n \rightarrow J_n$) by one of the conserved currents J_m and averaging over initial states with a Boltzmann distribution gives

$$\langle J_E J_m \rangle = \sum_n a_n \langle J_n J_m \rangle, \quad (53)$$

where we used the fact that $\langle J_E(t) J_m \rangle$ is independent of t . The a_n are therefore given by

$$a_n = \sum_l (C^{-1})_{nl} \langle J_E J_l \rangle, \quad (54)$$

where C is the matrix of correlations of the conserved currents

$$C_{nl} = \langle J_n J_l \rangle. \quad (55)$$

Squaring Eq. (52), and using Eqs. (53) and (54), gives

$$\begin{aligned} \lim_{t \rightarrow \infty} C_{J_E}(t) &\equiv \lim_{t \rightarrow \infty} \langle J_E(t_0) J_E(t_0 + t) \rangle \\ &= \lim_{t \rightarrow \infty} \left[\frac{1}{t} \int_0^t J_E(t') dt' \right]^2 \\ &= \sum_{n,m,l,k} (C^{-1})_{nl} \langle J_E J_l \rangle (C^{-1})_{mk} \langle J_E J_k \rangle C_{mn} \\ &= \sum_{k,l} \langle J_E J_l \rangle (C^{-1})_{lk} \langle J_E J_k \rangle, \end{aligned} \quad (56)$$

where we used $\sum_n C_{mn} C_{nl}^{-1} = \delta_{ml}$ to obtain the last line. Noting that J_E is odd under time reversal, only the odd conserved currents, $n = 1, 3, 5, \dots, N-1$, in Eq. (48) contribute.

We have investigated the validity of Eq. (56) numerically for sizes $N = 4, 6$, and 8 . All the numerical results in this paper are for parameter values $M = a = b = 1$ in the Toda Hamiltonian, Eq. (1). We prepare a large number (several thousand) of initial states appropriate to a temperature T (which we take to be $T = 0.5$) using standard Monte Carlo methods.³⁰ Starting from each of these states we perform molecular dynamics using a fourth-order symplectic algorithm,³¹ which combines high accuracy with long-term stability. We use a time step Δt equal to 0.05 .

Our results are presented in Figs. 4–6 for sizes $N = 4, 6$, and 8 , respectively. The solid line is the data for $C_{J_E}(t)$ and the (blue) dotted line is the RHS of Eq. (56) including all the (odd) currents. While the long time limit of $C_{J_E}(t)$ is close to the RHS of Eq. (56) there is a clear discrepancy.

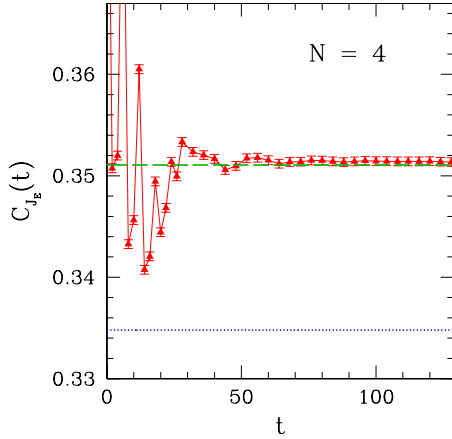


FIG. 4. (Color online) The correlation function of the energy current, defined in Eq. (51), as a function of time for $N=4$ particles. The (blue) short-dashed line is the RHS of Eq. (56) including all the (odd) Lax currents. There is a significant discrepancy with the long-time limit of $C_{J_E}(t)$. The (green) long-dashed line is the RHS of Eq. (56) including, in addition, all (odd) pairs of Lax currents. The agreement with the long-time limit of $C_{J_E}(t)$ is now excellent.

The discrepancy is removed if we note that the Lax currents J_n in Eq. (48) are not the only conserved currents but, in addition, *products* of these currents are conserved. This corresponds to enlarging the set of currents I_n in Eq. (52) to include bilinears $J_n J_l$.

Thus the leading correction to Eq. (56) will involve products of two currents $J_{nl} \equiv J_n J_l$, where one of the indices must be odd and the other even for J_{nl} to be odd under time reversal. Hence the total number of conserved “currents” to be included in the sums in Eq. (56) is $N/2$ (the odd J_n) plus $(N/2)^2$ the quadratic combinations with odd symmetry. Our results including the quadratic combinations of currents are shown by the (green) dashed line in Figs. 4–6. The agreement is now excellent. We thus see that the set of currents that are involved in the expansion must include not just the Lax currents but also products of these. We see that for the purpose of expanding an operator as in Eq. (52), the currents J_n are not a *linear* basis but rather J_E seems to be *algebraically* dependent on the J_n . Within the numerical scheme it is hard to determine if we have really saturated the persistent part by including just first and second powers of the Lax currents, but the remainder, if any, must be very small indeed.

We also test Eq. (52) for the case of $N=4$ by performing a least-squares fit to minimize

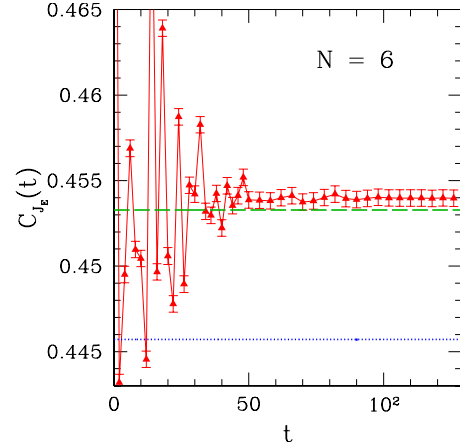


FIG. 5. (Color online) The same as Fig. 4 but for $N=6$.

$$\Delta J_E^2 \equiv \left\langle \left[\lim_{t \rightarrow \infty} \frac{1}{N_t} \sum_{t_m=1}^{N_t} J_E(t_m) - \sum_n a_n J_n \right]^2 \right\rangle \quad (57)$$

with respect to the a_n , where $t_m = m\Delta t$, and $N_t = t/\Delta t$ is the number of discrete times in the simulation. Including just the $N/2$ odd currents we find $\Delta J_E^2 = 0.016886$, which is not extremely small and represents the difference between the dotted (blue) line and the long-time limit of the data in Figs. 4–6. However, including $(N/2)^2$ quadratic combinations of currents that project on to the energy current we get a much lower value, $\Delta J_E^2 = 0.000220$, as expected from the good agreement between the dashed (green) line and the long-time limit of the data in Figs. 4–6. As a consistency check, we compare in Table I the fit coefficients obtained by minimizing Eq. (57) with those from Eq. (54) which used *equal time* Monte Carlo results. The agreement is good.

Mazur clarifies that the above expansion Eq. (52) should be valid for almost all initial conditions on the surface of constant energy. Here we have seen that, in addition, the expansion works to high numerical accuracy in the more general case of a canonical distribution.

VI. PERTURBED TODA RING AND DECAY RATES OF PERSISTENT CURRENTS

We have also studied numerically the decay of persistent currents when a small perturbation away from integrability is added to the Toda Hamiltonian. The technique is the same as that described above in Sec. V.

We consider two different perturbations

TABLE I. A comparison, for $N=4$, between the coefficients a_n in the expansion of the energy current in terms of the conserved currents, see Eq. (52). The “time-series” results were obtained by minimizing ΔJ_E^2 in Eq. (57). The “Monte Carlo” results were obtained from Eq. (54).

| | a_1 | a_3 | a_{12} | a_{14} | a_{32} | a_{34} |
|-------------|--------|---------|----------|----------|----------|----------|
| Time series | 0.4965 | -0.9626 | 0.1262 | -0.0591 | 0.0015 | 0.0178 |
| Monte Carlo | 0.4628 | -0.9412 | 0.1358 | -0.0681 | -0.0042 | 0.0227 |

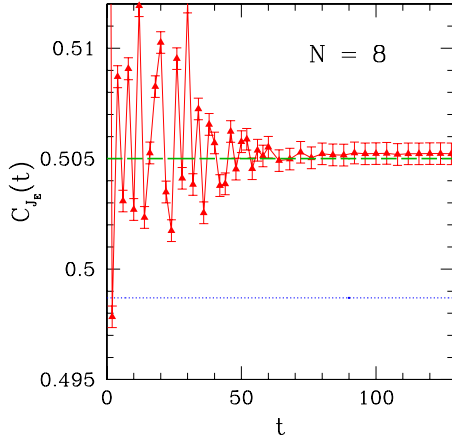


FIG. 6. (Color online) The same as Fig. 4 but for $N=8$.

$$\Delta\mathcal{H} = \begin{cases} \frac{w}{3} \sum_{n=1}^N (u_n - u_{n+1})^3 \\ \frac{v}{4} \sum_{n=1}^N (u_n - u_{n+1})^4. \end{cases} \quad (58)$$

The temperature is taken to be $T=1$, the time step to be $\Delta t = 0.02$, and the lattice has $N=64$ particles with periodic boundary conditions. We have verified that reducing Δt or increasing N did not make a significant difference to the results.

We compute the normalized correlation function of the conserved current J_3 , see Eq. (48c), defined by

$$C_3(t) = \frac{\langle J_3(t_0)J_3(t_0+t) \rangle}{\langle (J_3)^2 \rangle}. \quad (59)$$

In the absence of any perturbation which breaks integrability, w or v in Eq. (58), $C_3(t)$ is equal to unity. It is also equal to unity at $t=0$ for any Hamiltonian. Figure 7 shows data for $C_3(t)$ for the cubic perturbation in Eq. (58), for several values of the strength of the perturbation w . As expected the J_3 correlation function decays to zero on a time scale which decreases with increasing w .

We assume that the data fits the scaling form

$$C_3(t) = \tilde{C}_3(tw^\phi), \quad (60)$$

where ϕ is a crossover exponent indicating that w is a ‘‘relevant’’ perturbation for the integrable model. Figure 8 shows scaled data for the cubic perturbation in Eq. (58) assuming $\phi=1.9$ which gives the best data collapse for the largest sizes.

However, as shown in Fig. 9 it is also possible that the data for even larger sizes will collapse for $\phi=2$. The result $\phi=2$ (in a quantum version) follows from Fermi’s golden rule. It is commonly encountered in quantum integrable systems,²⁸ where the current decays due to the addition of a term V in the Hamiltonian that destroy integrability. The Fermi golden rule states that the decay rate of a state i is given, to lowest order, by

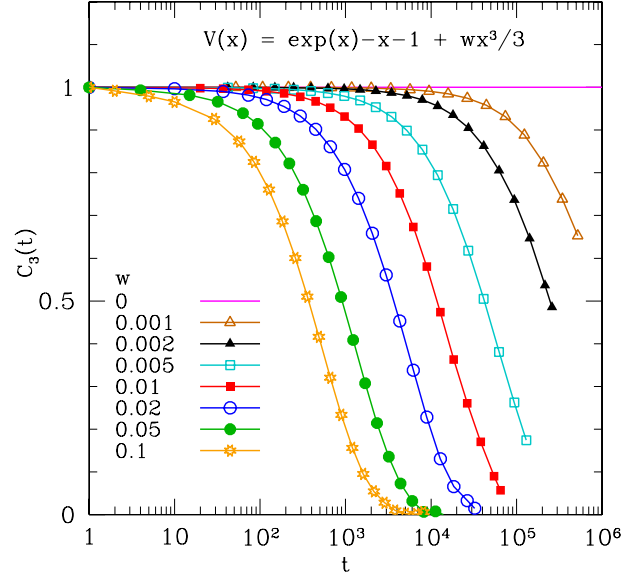


FIG. 7. (Color online) The normalized correlation function, defined in Eq. (59), for the current J_3 , for several values of the cubic perturbation w in Eq. (58) added to the integrable Toda Hamiltonian. The size is $N=64$. Including the perturbation, the system is no longer integrable, so the correlation function tends to zero on a time scale which diverges as $w \rightarrow 0$.

$$\frac{1}{\tau} = \frac{2\pi}{\hbar} \sum_j | \langle i | V | j \rangle |^2 \delta(\epsilon_j - \epsilon_i). \quad (61)$$

This may be interpreted as the decay rate of a current or a quasiparticle that is infinitely long lived in the integrable case. Hence we expect that an integrable current analogous to J_n , and its correlations would decay in this fashion, whereby we expect $\phi=2$.

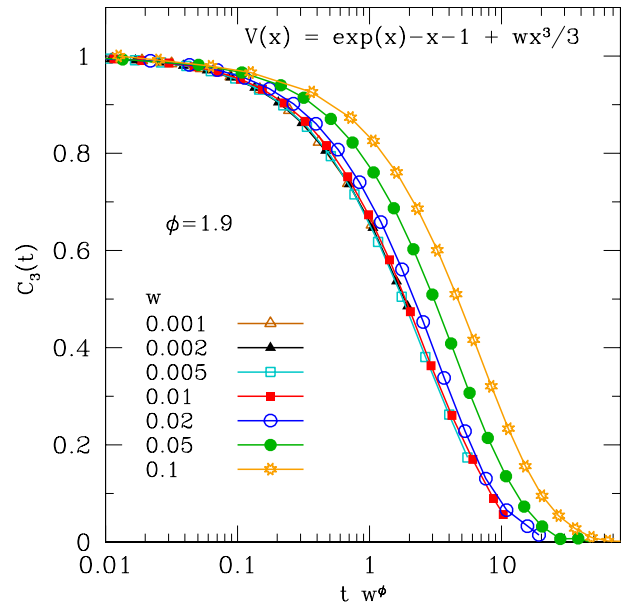


FIG. 8. (Color online) A scaling plot, according to Eq. (60), of the data in Fig. 7, with crossover exponent $\phi=1.9$ which gives the best data collapse for small w .

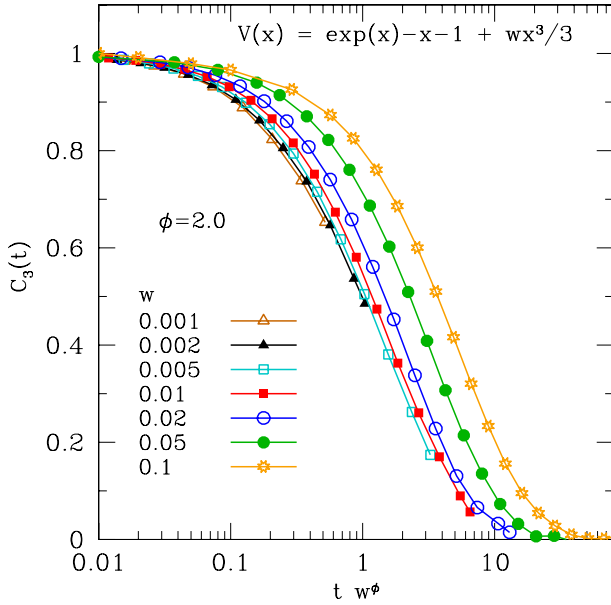


FIG. 9. (Color online) Same as Fig. 8 but for $\phi=2$, which is the expected result as discussed in the text. It is plausible that this value of ϕ will give good data collapse in the scaling limit $w \rightarrow 0, t \rightarrow \infty$. This asymptotic regime is reached only for very small values of w (and correspondingly very long times) indicating that corrections to scaling are large.

We note that the data in Fig. 9 only collapses for very small values of w and very large times, indicating that “corrections to scaling” are large.

We have also studied the effect of the quartic perturbation in Eq. (58) and show the unscaled data in Fig. 10. We expect the same crossover exponent ϕ for the quartic perturbation as for the cubic perturbation and indeed the data is consistent with the asymptotic exponent being $\phi=2$ as shown in Fig. 11.

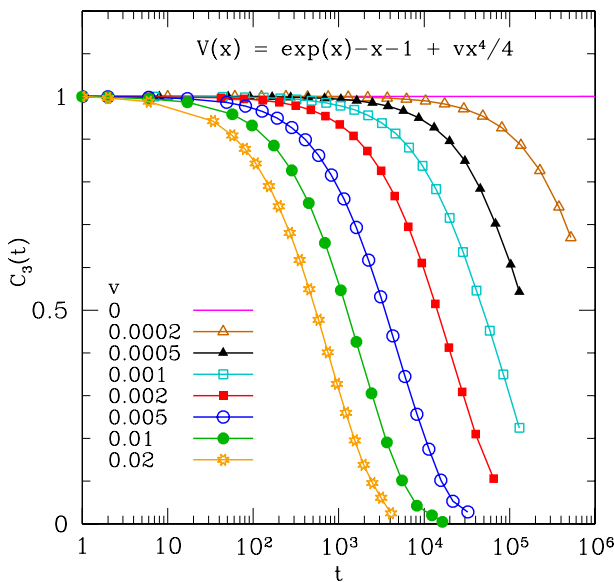


FIG. 10. (Color online) The same as Fig. 7 but for the quartic perturbation v in Eq. (58).

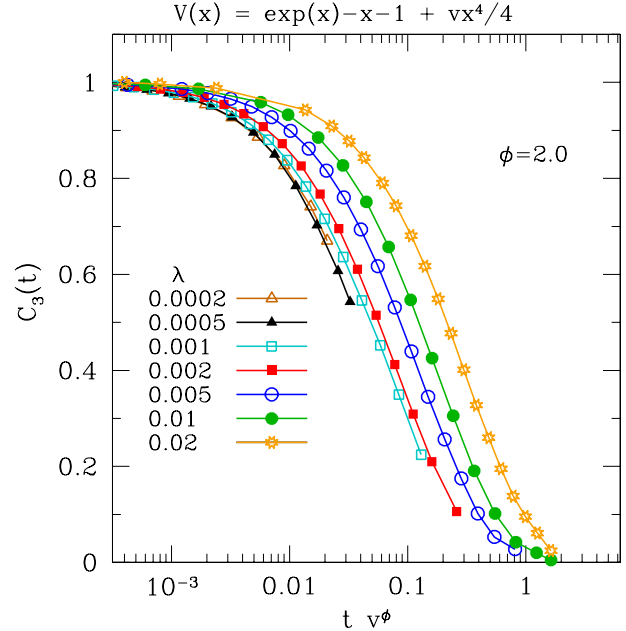


FIG. 11. (Color online) A scaling plot with $\phi=2$, as in Fig. 9, but for the quartic perturbation v in Eq. (58).

VII. CONCLUSIONS

In this paper we have shown that the result of Toda for the frequency of the cnoidal waves of the Toda lattice is only correct for weak anharmonicity or long wavelength. We give a general expression for the frequency, as well as results for the average kinetic energy and mean square displacement in the Toda ring. The distinction between the dispersion relation of Toda, Eq. (B7), and the one found here, Eq. (16), is important only in the limit of large wave vectors and high anharmonicity—in all other cases it is negligible.

In addition, we have discussed the conserved currents of the Toda model in some detail. In particular, we showed numerically that the persistent part of general currents can be expressed in terms of the conserved currents according to Eq. (52), provided one includes not only the Lax currents but also quadratic combinations of the Lax currents (which are, of course, also conserved). Finally, we have studied the decay of the conserved currents when a perturbation is added to the model which destroys integrability. The time scale for decay is governed by a crossover exponent ϕ . Our numerical data is consistent with the value $\phi=2$, which can also be obtained by Fermi golden rule-type arguments.

ACKNOWLEDGMENTS

We acknowledge support from the NSF under Grants No. DMR-0706128 (B.S.S.) and No. DMR-0906366 (A.P.Y.). We thank Bill Sutherland for sharing his unpublished notes on the periodic case with us. His solution (Ref. 16) has the same form that we report in Eq. (16).

APPENDIX A: ELLIPTIC THETA FUNCTIONS AND INTEGRALS

The most convenient version of these functions is given in Whittaker and Watson, Chapter XXI (Ref. 9) and Abramow-

itz and Stegun.³² We note here the definitions of the required theta functions and their Fourier series

$$\begin{aligned}
 q &= e^{-\pi K'/K}, \\
 \theta_4(z) &= 1 + 2 \sum_{n=1}^{\infty} (-1)^n q^{n^2} \cos(2nz), \\
 K &\equiv K(m) = \int_0^{\pi/2} dx \sqrt{1 - m \sin^2 x}, \\
 \theta_1(z) &= 2 \sum_{n=0}^{\infty} (-1)^n q^{(n+1/2)^2} \sin(2n+1)z, \\
 K' &= K(1-m), \\
 \theta_2(z) &= 2 \sum_{n=0}^{\infty} q^{(n+1/2)^2} \cos(2n+1)z, \quad (\text{A1}) \\
 E &= \int_0^{\pi/2} dx \sqrt{1 - m \sin^2 x}, \\
 \theta_3(z) &= 1 + 2 \sum_{n=1}^{\infty} q^{n^2} \cos(2nz). \quad (\text{A2})
 \end{aligned}$$

We note that for small anharmonicity, all the elliptic functions can be expanded equivalently in terms of the parameter m or the nome q . These expansions are related since we may expand

$$q = \frac{1}{16}m + \frac{1}{32}m^2 + \frac{21}{1024}m^3 + \frac{31}{2048}m^4 + O(m^5). \quad (\text{A3})$$

We note that as $m \rightarrow 1$, $K(m) \sim \log\{\frac{4}{\sqrt{1-m}}\}$, and $E(m) \sim \frac{\pi}{2}$. Further, as $m \rightarrow 1$, the theta functions are more easily calculated by using the Jacobi transformation⁹ (p 475), where we display the parameter m

$$\theta_n(z|m) = c_n \frac{K}{K'} e^{-\{z^2(K/\pi K')\}} \theta_n\left(i \frac{K}{K'} z|m\right) \quad (\text{A4})$$

with $c_1 = -i$ and the remaining $c_j = 1$. For computing the soliton spectrum, we will need the expression for $n=1$

$$\begin{aligned}
 \theta_1(z|m) &= 2 \frac{K}{K'} e^{-\{z^2(K/\pi K')\}} \sum_{n=0}^{\infty} (-1)^n e^{-\pi(K/K')(n+1/2)^2} \\
 &\quad \times \sinh(2n+1) \frac{K}{K'} z. \quad (\text{A5})
 \end{aligned}$$

APPENDIX B: TODA'S CNOIDAL WAVE FREQUENCY CALCULATION, DUALITY, AND BOUNDARY CONDITIONS

Consider N atoms in one dimension, with displacements u_1, u_2, \dots, u_N , which we call the bulk displacements. Addi-

tionally, there are two ‘‘boundary’’ atoms, atom 0 to the left of atom 1, and atom $N+1$ to the right of atom N . Here we do not assume periodic boundary conditions but instead consider two different types of boundary conditions: (1) ‘‘clamped’’ boundary conditions for which $u_0 = u_{N+1} = 0$ (2) and ‘‘open’’ boundary conditions for which, it turns out, we will need $u_0 = u_1$ and $u_{N+1} = u_N$. We will actually focus on ‘‘mixed’’ boundary conditions, i.e., free at one end and clamped at the other.

The interaction between two atoms is represented by a nearest-neighbor term $V(u_j - u_{j-1})$ with a suitable function V , the exponential interaction as in Eq. (1), or a harmonic term for comparison. The Lagrangian is

$$L = \frac{1}{2M} \sum_{j=1}^N \dot{u}_j^2 - \sum_{j=J_l}^{J_r} V(u_j - u_{j-1}), \quad (\text{B1})$$

where $J_l=1$ (2) for clamped (open) boundary conditions at the left and $J_r=N+1$ (N) for a clamped (open) boundary conditions at the right. Even for open boundary conditions, the boundary sites do not have any kinetic energy since they are ‘‘fictitious,’’ i.e., are simply there to impose the necessary boundary conditions.

We introduce the particle separations $r_j = u_j - u_{j-1}$ as new generalized coordinates, these and their canonically conjugate momenta s_j found below, are the ‘‘dual variables’’ of Toda. It follows that the inverse relations are $u_j = \sum_{l=1}^j r_l$. The kinetic energy is expressible in terms of the time derivatives, \dot{r}_j . The canonically conjugate ‘‘momenta’’ to the r_j are $s_j = \frac{\partial H}{\partial \dot{r}_j} = M \sum_{l=j}^N \dot{u}_l$, whereby, for $1 \leq j \leq N-1$, we get $M \dot{u}_j = s_j - s_{j+1}$, and $s_N = M \dot{u}_N$. Thus we obtain the Hamiltonian in terms of the dual variables as

$$H = \frac{1}{2M} \sum_{j=1}^{N-1} (s_j - s_{j+1})^2 + \frac{1}{2M} s_N^2 + \sum_{j=J_l}^{J_r} V(r_j). \quad (\text{B2})$$

Hamilton’s equations of motion are therefore now

$$\begin{aligned}
 \dot{r}_j &= \frac{1}{M} (2s_j - s_{j-1} - s_{j+1}), \quad \dot{s}_j = - \frac{\partial V(r_j)}{\partial r_j} \\
 &\quad \text{for } 2 \leq j \leq N-1. \quad (\text{B3})
 \end{aligned}$$

The case of a clamped right boundary is complicated to deal with so we will always choose it to be open. We therefore have $J_r=N$, and the kinetic energy term of the N th atom is written as $\frac{1}{2M} (s_N - s_{N+1})^2$ with $s_{N+1}=0$ as the boundary condition *at all times*, so that the equation Eq. (B3) is extended to $j=N$.

On the left side boundary, the clamped case with $J_l=1$ can be dealt with easily by extending Eq. (B3) to $j=1$ by introducing an s_0 and requiring that $s_0 = s_1$ so Eq. (B3) has the same form for $j=1$ as for $j>1$. The open case on the left boundary has a missing $V(r_1)$ in the potential energy so that r_1 is a cyclic coordinate (so $\ddot{r}_1=0$) and we must require $s_1 = \text{constant}$.

For the case of the harmonic chain, these boundary conditions are easily imposed on the solution $e^{\pm i\omega_k t} \cos(kr_j + \delta)$

and one reproduces the various integer and half integer quantization of the wave vector k . We note that the solutions are not traveling waves but rather products of functions of space and time since in all cases here we must set the boundary variables to be time-independent constants.

For the Toda lattice, we choose $V(r_j) = \frac{a}{b}(e^{-br_j} - 1 + br_j)$ so that the equations of motion Eq. (B3) are written for the typical case of left-clamped and right-open boundaries

$$\frac{\ddot{s}_j}{a + s_j} = \frac{b}{M}[s_{j-1} + s_{j+1} - 2s_j], \quad 1 \leq s_j \leq N,$$

and $s_0 = s_1, \quad s_{N+1} = 0.$ (B4)

The remarkable insight of Toda in solving this equation, was apparently inspired by seeing an addition identity of the Jacobian zeta function $Z[u]$ that we met earlier in Eq. (20). The salient features of this function are as follows: periodicity $Z[u + 2K] = Z[u]$, parity $Z[-u] = -Z[u]$, and hence nodes at $Z[0] = 0 = Z[K]$. The relevant identity is¹⁹

$$Z[u + v] + Z[u - v] - 2Z[u] = \frac{Z''[u]}{Z'[u] + \frac{E}{K} - 1 + \frac{1}{\text{sn}^2(v)}}. \tag{B5}$$

Comparing Eq. (B4) and (B5), one sees that these are very similar, provided we make the hypothesis that Eq. (B4) should collapse to an ordinary differential-difference equation. Thus we are obliged to combine the space and time dependence into a single variable $\phi_j = kj - \omega t + \delta$, and this helps in solving the Eq. (B4) for the bulk. We thus can only solve for traveling waves. However, it makes it impossible to satisfy the boundary conditions, since the latter involve time independent vanishing of certain constants. With Toda, we will ignore the boundary terms and write down the solution for s_j that is implied by Eq. (B5). With a scale factor $\frac{\phi}{K}$ we relate u and ϕ as $u = \frac{\phi}{\pi}K$ so that increasing u by its natural periodicity $2K$ winds the phase by 2π . Then we see that $\frac{d}{dt} = -\frac{K}{\pi}\omega \frac{d}{du}$, and $j \rightarrow j+1$ increases $u \rightarrow u + \frac{kK}{\pi}$ whence $v = \frac{kK}{\pi}$. The mapping is complete with a scale factor relating s_j to $Z[u]$ and determining ω as a function of k gives the two Toda solutions

$$s_j(t) = \mp \frac{M}{b} \left(\frac{K\omega_k^T}{\pi} \right) Z \left[\frac{K}{\pi} (kj \mp \omega_k^T t + \delta) \right], \tag{B6}$$

$$\omega_k^T = \sqrt{\frac{ab}{M} \frac{\pi}{K} \frac{1}{\sqrt{\frac{E}{K} - 1 + \frac{1}{\text{sn}^2\left(\frac{kK}{\pi}\right)}}}}. \tag{B7}$$

Using $M\dot{u}_j = s_j - s_{j+1}$ and the expression Eq. (20), and integrating once we find the displacement in terms of the theta functions

$$u_j = \frac{1}{b} \log \frac{\theta_4 \left[\frac{1}{2} (kj \mp \omega_k^T t + \delta) \right]}{\theta_4 \left[\frac{1}{2} [k(j+1) \mp \omega_k^T t + \delta] \right]} \tag{B8}$$

in agreement with our Eq. (10).

In Sec. II C we showed that the same functional form as Eq. (B8) describes oscillatory solutions with periodic boundary conditions but with a different expression for the frequency, Eq. (16), in place of Eq. (B6). This situation requires a few clarifying remarks.

(a) Equation (B6) is in a traveling wave form, and since we cannot superpose two non linear waves, e.g., with the two signs of the time dependence, this prevents us from satisfying the various boundary conditions (clamped and open) discussed above. Thus the Toda dispersion relation is *not the solution of the problem he starts with*.

(b) The spectra in Eqs. (16) and (18) are very close for small wave vectors, or for small values of the parameter “ m ,” i.e., for weak anharmonicity. Figure 1 illustrates the two dispersions.

(c) A reader might wonder if Eqs. (B7) and (16) are not actually identical, with the help of some obscure identity, e.g., in Ref. 9. However, this cannot be the case for two reasons. One is mathematical. While the expression in Eq. (B6) is doubly periodic in the complex k plane, the expression in Eq. (16) is not—the θ functions have periodicity factors attached for translations along the imaginary axis. The other reason is physical. If the two expressions were somehow identical, the potential energy average Eq. (D3) would be identically zero for the periodic system, which is impossible since $V(x) \geq 0$ with the equality only at $x=0$.

(d) Toda is correct to take the functional form in Eq. (B6) seriously. However for periodic boundary conditions, the correct frequency of the cnoidal wave is not the one in Toda’s works,¹ but rather Eq. (16), which appears here for the first time, to the best of our knowledge. Toda’s solution is only correct in the limit of weak anharmonicity or long wavelength.

APPENDIX C: ALTERNATE DERIVATION OF THE SOLUTION WITH PERIODIC BOUNDARY CONDITIONS

In this appendix we give an alternative derivation of the dispersion relation of the Toda ring in Eq. (16) by substituting the Fourier series in the second line of Eq. (23) into Eq. (9). Taking the second derivative of this with respect to ϕ we obtain

$$\text{LHS Eq.(9)} = 4\bar{\omega}_k^2 \sum_{n=1}^{\infty} n \frac{q^n}{1 - q^{2n}} \sin n \left(\phi - \frac{k}{2} \right) \sin n \frac{k}{2}. \tag{C1}$$

To obtain the expansion of the RHS of Eq. (9) we start with Eq. (23) and use the Fourier expansion of sn^2 due to Jacobi³³ (again)

$$\text{sn}^2\left(\frac{2K}{\pi}x\right) = \frac{1}{m} \left\{ 1 - \frac{E}{K} \right\} - \frac{2\pi^2}{mK^2} \sum_{n=1}^{\infty} n \frac{q^n}{1-q^{2n}} \cos 2nx. \quad (\text{C2})$$

Thus we find

$$\begin{aligned} \text{RHS Eq. (9)} &= \frac{4\pi^2}{\sqrt{m}K^2} \frac{\theta_1^2\left(\frac{k}{2}\right)}{\theta_4^2(0)} \sum_{n=1}^{\infty} n \frac{q^n}{1-q^{2n}} \\ &\quad \times \sin n\left(\phi - \frac{k}{2}\right) \sin n\frac{k}{2}. \end{aligned} \quad (\text{C3})$$

The series in Eqs. (C1) and (C3) are seen to be identical with the choice of the dispersion in Eq. (16).

APPENDIX D: POTENTIAL ENERGY OF THE TODA RING

Let us rewrite the potential energy term Eq. (11) with ϕ representing any one phase factor

$$\begin{aligned} e^{bu_n - bu_{n+1}} &= e^{d_k(\phi) - d_k(\phi+k)} = \frac{1}{\theta_4^2(0)} \left\{ \theta_4^2\left(\frac{k}{2}\right) - \theta_1^2\left(\frac{k}{2}\right) \frac{\theta_1^2\left(\frac{\phi}{2}\right)}{\theta_4^2\left(\frac{\phi}{2}\right)} \right\}, \\ &= \frac{1}{\sqrt{m}} \frac{\theta_1^2\left(\frac{k}{2}\right)}{\theta_4^2(0)} \left\{ \frac{1}{\text{sn}^2\left(\frac{kK}{\pi}\right)} - m \text{sn}^2\left(\frac{K}{\pi}\phi\right) \right\}, \\ &= \bar{\omega}_k^2 \frac{K^2}{\pi^2} \left\{ \frac{1}{\text{sn}^2\left(\frac{kK}{\pi}\right)} - m \text{sn}^2\left(\frac{K}{\pi}\phi\right) \right\}. \end{aligned} \quad (\text{D1})$$

We used the dispersion relation for the ring, Eqs. (16) to proceed in this equation.

We now recall $\phi = \omega_k t$ and average this expression over a single cycle in time, (i.e., $\int_0^{T_k} \dots dt$, where $T_k = \frac{2\pi}{\omega_k}$), or $u = \frac{K}{\pi}\phi$, with $0 \leq u \leq 2K$. We ignore the site index, since each atom has the same average value. We use

$$\frac{1}{2K} \int_0^{2K} du \text{sn}^2(u) = \frac{1}{m} \left(\frac{E}{K} - 1 \right)$$

so that the time average of this term can be written using the expression Eq. (B7) as

$$e^{d_k(\phi) - d_k(\phi+k)} = \left(\frac{\bar{\omega}_k}{\bar{\omega}_k^T} \right)^2 \quad (\text{D2})$$

and thus the potential energy average over a cycle is

$$\overline{\text{PE}} = N \frac{a}{b} \left[\left(\frac{\bar{\omega}_k}{\bar{\omega}_k^T} \right)^2 - 1 \right]. \quad (\text{D3})$$

¹M. Toda, *J. Phys. Soc. Jpn.* **22**, 431 (1967); **23**, 501 (1967); *Suppl. Prog. Theor. Phys.* **36**, 113 (1966)
²M. Toda, *Phys. Scr.* **20**, 424 (1979).
³M. Sataric, J. A. Tuszynski, R. Zakula, and S. Zekovic, *J. Phys.: Condens. Matter* **6**, 3917 (1994).
⁴V. Muto, A. C. Scott, and P. L. Christiansen, *Physica D* **44**, 75 (1990).
⁵F. d'Ovivio, H. G. Bohr, and P. Lindgard, *J. Phys.: Condens. Matter* **15**, S1699 (2003).
⁶M. Hénon, *Phys. Rev. B* **9**, 1921 (1974).
⁷H. Flaschka, *Phys. Rev. B* **9**, 1924 (1974).
⁸B. S. Shastry and A. P. Young, e-print [arXiv:1007.1173](https://arxiv.org/abs/1007.1173).
⁹E. Whittaker and G. N. Watson, *Modern Analysis*, 4th ed. (Cambridge University Press, Cambridge, U. K., 1988).
¹⁰B. Sutherland, *Rocky Mountain J. Math.* **8**, 413 (1978).
¹¹M. Gutzwiller, *Ann. Phys. (N.Y.)* **133**, 304 (1981).
¹²E. Sklyanin, *Nonlinear Equations in Classical and Quantum Field Theory*, edited by N. Sanchez, Lecture Notes in Physics Vol. 226 (Springer-Verlag, Berlin, 1985).
¹³V. Pasquier and M. Gaudin, *J. Phys. A* **25**, 5243 (1992).
¹⁴R. Siddharthan and B. S. Shastry, *Phys. Rev. B* **55**, 12196

(1997).

¹⁵M. Toda, *Theory of Nonlinear Lattices* (Springer-Verlag, Berlin, 1981).
¹⁶B. Sutherland (unpublished).
¹⁷The mass is denoted by M rather than m , to avoid confusion with the Elliptic function parameter.
¹⁸We will always denote the elliptic functions by the parameters $m=k^2$ and $m'=1-m=1-k'^2=k'^2$ rather than by their modulus k, k' (in order to avoid confusion with the symbol for the wave vector).
¹⁹Reference 9 problem 1, Chap. 21.9, page 487.
²⁰I. S. Gradshteyn and I. M. Ryzhik, *Tables of Integrals, Series and Products*, (Academic, New York, 1980), p. 923, Sec. 8.191.
²¹This result follows most simply from the Fourier series of both sides.
²²Reference 9 and Chapter 21.41, page 470, and example 3, Chapter 21.61, page 479.
²³Equation (21) is well known, e.g. see Eq. (17.4.38) of Ref. 32. The useful identity Eq. (22) is however not listed in literature as far as we could find and it seems worth stating its derivation. Here the Poisson summation formula is very useful, and gives

Eq. (22) from Eq. (21) in a few lines. We first write Eq. (21) after adding and subtracting the $n=0$ term as

$$Z(u) = -\frac{\pi u}{2KK'} + \frac{\pi}{2K} \sum_{n=-\infty}^{\infty} \frac{\sin \frac{n\pi u}{K}}{\sinh \frac{n\pi K'}{K}}.$$

Since this is in the form of a Fourier “sine series,” we use the “sine-transforms” version of the Poisson summation formula

$$\sum_{n=-\infty}^{\infty} g(n) \sin \frac{n\pi u}{u_0} = u_0 \sum_{\nu=-\infty}^{\infty} \hat{g}(u - 2\pi u_0 \nu),$$

$$\text{where } \hat{g}(x) = \int_{-\infty}^{\infty} dy \sin(xy) g(u_0 y)$$

with $u_0 = K/\pi$ and $g(n) = \frac{\pi}{2K} \frac{1}{\sinh(\pi K' n/K)}$, yielding the required result. Similarly Eq. (23) for the displacement is not listed in literature. It may be obtained by a similar analysis as the above series, or alternately from Eq. (22) by an integration

with respect to the parameter ϕ' as given in the first line.

²⁴This follows since in the limit $m \rightarrow 1$, $k \rightarrow 0$, we have the behavior $\text{sn}(kK/\pi) \rightarrow \sinh(kK/\pi)$, $\text{cn}(kK/\pi) \rightarrow 1$, and $E \rightarrow 1$, $a \rightarrow 1$, and we take into account Eq. (30).

²⁵Here k stands for the wave vector and should not be confused with the elliptic function modulus used in standard books (Ref. 9). As mentioned earlier, we will use the elliptic parameter m consistently in this work and not the elliptic modulus “ k .”

²⁶Reference 32, Identity 17.3.23, page 591.

²⁷P. Mazur, *Physica* **43**, 533 (1969).

²⁸P. Jung and A. Rosch, *Phys. Rev. B* **76**, 245108 (2007), older articles are referred to here.

²⁹T. Niemeijer, *Physica* **36**, 377 (1967).

³⁰M. E. J. Newman and G. T. Barkema, *Monte Carlo Methods in Statistical Physics* (Oxford University Press, Oxford, 2002).

³¹I. Omelyan, I. Mryglod, and R. Folk, *Comput. Phys. Commun.* **146**, 188 (2002).

³²M. Abramowitz and I. Stegun, *Handbook of Mathematical Functions*, (Dover, New York, 1972), p. 577, Identity 16.30.4.

³³Reference 9, Chapter 22, page 520, example 5.